A R C H I V E S O F M E T A L L U R G Y A N D M A T E R I A L S
Volume 50 2005 Issue 4

R. REJSZEK*, P. MACIOŁ*, J. WYPARTOWICZ*

MATHEMATICAL MODELLING OF SOLIDIFICATION OF IRON CONTAINING OXYGEN WITH THE CONTRIBUTION OF SURFACE CONVECTION

MODEL MATEMATYCZNY KRZEPNIĘCIA ŻELAZA ZAWIERAJĄCEGO TLEN Z UWZGLĘDNIENIEM KONWEKCJI POWIERZCHNIOWEJ

Oxygen is the surface active component of steel. Its uneven distribution in the vicinity of solid-liquid boundary during solidification is the reason of surface convection, which, in addition to free (temperature driven) and forced convection is the third mode of heat and mass transfer. This work presents an attempt of mathematical modelling of metal solidification with the contribution of surface convection. The cylindrical sample of iron with free surface of liquid phase contained in crucible was chosen as the calculation domain. This sample was subjected to a slow crystallization with radial heat transfer, at which the oxygen dissolved in liquid iron was accumulated in the region of solid-liquid boundary due to segregation. Oxygen concentration gradient resulted in surface (Marangoni) convective flow. Mathematical model consisted of the equations of continuity, momentum balance, thermal energy balance and oxygen mass balance in convective-diffusive flow. Shear stress resulting from concentration gradient and temperature gradient was introduced as a boundary condition. As a result of numerical calculations, executed by means of ADINA-F® program, the temperature, concentration and velocity fields were determined as a function of time. The Marangoni flow was found to be active generally in opposite direction to thermal convection flow and its action was restricted to small surface area in the neighbourhood of advancing freezing front.

Tlen jest powierzchniowo aktywnym składnikiem stali, a jego nierównomierny rozkład w sąsiedztwie granicy faza stała – faza ciekła powoduje konwekcję powierzchniową, która jest dodatkowym, oprócz konwekcji swobodnej i wymuszonej, sposobem transportu ciepła i masy. W obecnej pracy przedstawiono próbę matematycznego modelowania procesu krzepnięcia metalu z udziałem konwekcji powierzchniowej. Domenę obliczeniową stanowiła cylindryczna próbka ciekłego żelaza o swobodnej powierzchni, znajdującego się w tyglu. Została ona poddana powolnej krystalizacji z radialnym odprowadzeniem ciepła, przy której tlen rozpuszczony w ciekłym żelazie gromadził się przed frontem krzepnięcia na skutek

* WYDZIAŁ INŻYNIERII METALI I INFORMATYKI PRZEMYSŁOWEJ, AKADEMIA GÓRNICZO-HUTNICZA, 30-059 KRAKÓW, AL. MICKIEWICZA 30

segregacji. Gradient stężenia tlenu powodował konwekcję powierzchniową (Marangoniego). Model matematyczny zawierał równanie ciągłości, bilansu pędu, bilansu energii cieplnej i bilansu masy tlenu w przepływie konwekcyjno-dyfuzyjnym. Naprężenie styczne wywołane gradientem stężenia i temperatury zostało wprowadzone jako warunek brzegowy. W wyniku obliczeń numerycznych zrealizowanych za pomocą programu ADINA-F® wyznaczono pola temperatury, stężenia i prędkości w funkcji czasu. Przepływ Marangoniego zachodzi w kierunku przeciwnym do temperaturowego przepływu konwekcyjnego, a jego oddziaływanie ogranicza się do małego fragmentu powierzchni w pobliżu przemieszczającego się frontu krzepnięcia.

1. Introduction

The analysis of the processes of metal melting and solidification requires the solution of numerous problems of heat and mass transfer. The complete description of mass transfer should consider diffusion of components in the liquid and solid phase, convective flow resulting from the temperature or concentration field as well as the flow forced through the energy introduced into the system, e.g. the mechanical energy of liquid metal jet during casting or magnetic field energy applied for metal stirring and stabilization of its surface. However, the flow resulting from the surface convection is usually not included into this description. It originates from local differences in surface or inter-phase tension.

In the conditions typical for high temperature metallurgical processes three main driving forces of surface convection may be distinguished: gradient of temperature field $\partial T/\partial x$, gradient of concentration of surface active elements $\partial C/\partial x$, and the electric potential gradient $\partial \Phi/\partial x$, which for example may occur at the molten salt – liquid metal interface in the electrolytic cell due to the difference in current density. The resulting shear stress may be expressed as follows:

$$\tau = \mu \frac{\partial u}{\partial z} = \left(\frac{\partial \sigma}{\partial T} \cdot \frac{\partial T}{\partial x}\right)_{C,\phi} + \left(\frac{\partial \sigma}{\partial C} \cdot \frac{\partial C}{\partial x}\right)_{T,\phi} + \left(\frac{\partial \sigma}{\partial \phi} \cdot \frac{\partial \phi}{\partial x}\right)_{T,C}. \tag{1}$$

In the present work the effect of electric potential is not considered. The surface convection flow (Marangoni flow) may cause considerably strong movements of free surface of liquid metal during crystallization, and, consequently, modify the shape of inter-phase boundary.

Mathematical modelling of processes with the contribution of surface convection is actually in the early stage of development. So far only simple cases are quantitatively characterized, as the surface convection during melting of iron containing oxygen [1] or nitrogen introduction into liquid iron [2]. Present work deals with the case of crystallization the cylindrical sample of liquid iron containing initially 0.002 mass % of oxygen. The abundant evolution of oxygen at the front of crystallization results in the shear force at liquid metal surface. The work is aimed at the determination, how the surface convection influences the velocity field, the temperature field and concentration field in liquid, and how these changes result in total crystallization rate.

2. Surface convection — Marangoni flow

The effect of oxygen concentration and temperature on the surface tension of iron is the starting point in the calculation of heat and mass transfer during crystallization. This is presented in simple expression worked out by Chung and Cramb [3] on the basis of Belton [4] equation:

$$\sigma = 1.913 - 0.00043 \cdot (T - 1823) - 0.000153 \cdot T \cdot \ln(1 + K_O \cdot C), \quad (2)$$

where:

$$\log K_O = \frac{11370}{T} - 4.09, \quad (3)$$

K_O — adsorption coefficient for oxygen on liquid iron,
σ — surface tension, N/m
C — oxygen concentration, mass pct.

The dependence of surface tension of temperature and oxygen concentration is presented in Fig. 1. It may be seen, that for pure iron and low oxygen concentrations

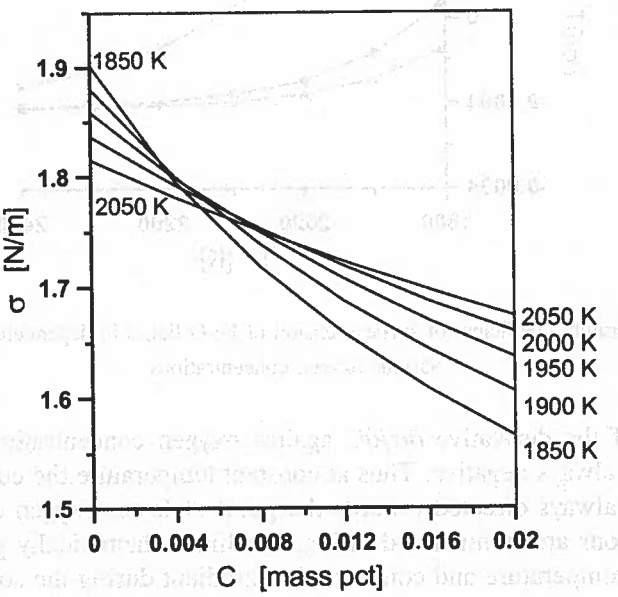

Fig. 1. Surface tension of Fe-O liquid in dependence on temperature and oxygen concentration, calculated from [3] and [4]

the surface tension lowers with rising temperature. For higher oxygen concentrations the opposite trend may be observed. Thus, if constant temperature is assumed, the increase in oxygen content in Fe-O solution lowers its surface tension. If the temperature varies from point to point within the sample, the cumulated effect of concentration and

temperature depends on the local values of these parameters. This effect is illustrated in Fig. 2, where the value of the derivative $\partial\sigma/\partial T$ is plotted against temperature for various oxygen concentrations: 0.001, 0.002 and 0.018 mass %. For the lowest oxygen concentration the derivative $\partial\sigma/\partial T$ is always negative, what means, that the surface convective movement is always directed from the point of higher temperature towards the lower temperature. If the oxygen concentration is 0.018 mass %, the convective surface flow is always directed from lower to higher temperature. At oxygen concentration 0.002 mass % the temperature 1827 K is the inversion point between positive and negative value of the $\partial\sigma/\partial T$ derivative. This means, that at this temperature the surface flow reverses its direction.

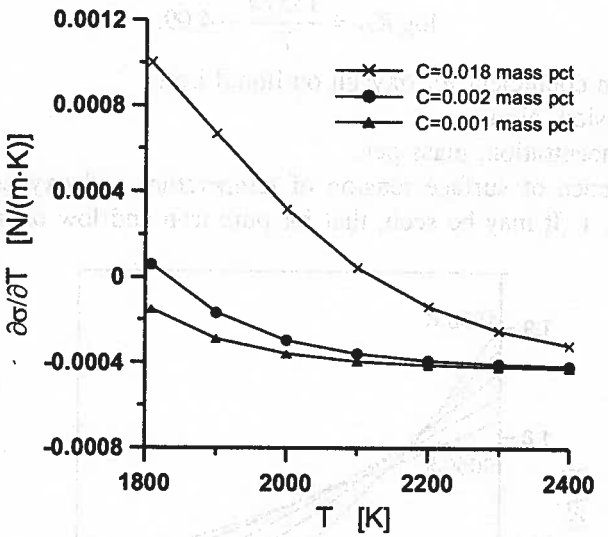

Fig. 2. The temperature coefficient of surface tension of Fe-O liquid in dependence on temperature for various oxygen concentrations

The plot of the derivative $\partial\sigma/\partial C$ against oxygen concentration (Fig. 3) reveals, that its value is always negative. Thus at constant temperature the concentration driven surface flow is always directed towards the point of lower oxygen concentration. The above observations are summarized in Fig. 4, which schematically presents the cumulative effect of temperature and concentration gradient during the solidification of iron containing oxygen.

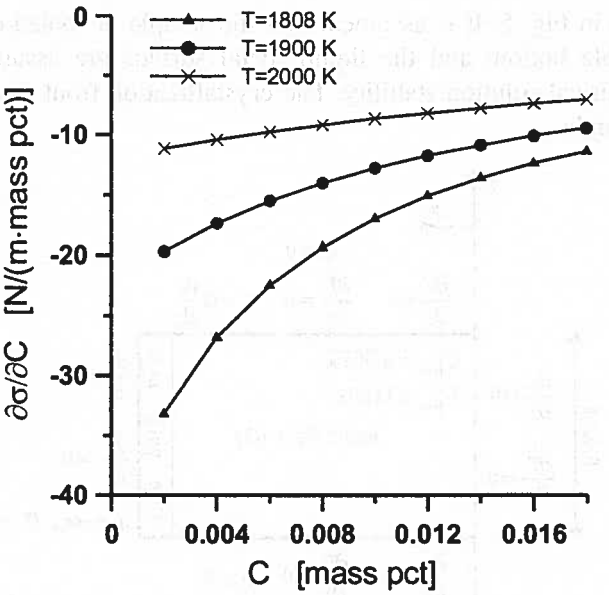

Fig. 3. The concentration coefficient of surface tension of Fe-O liquid in dependence on oxygen concentration for various temperatures

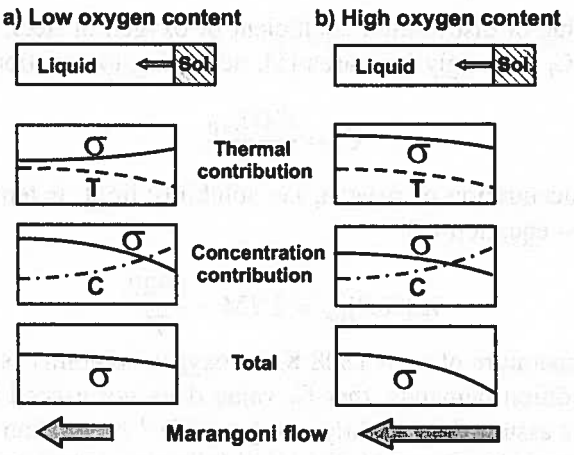

Fig. 4. Schematic representation of cumulative effect of temperature and oxygen concentration gradients on the direction of surface convective flow in the Fe-O liquid during solidification a) low oxygen content, b) high oxygen content

3. Mathematical model of the crystallization of iron containing oxygen

The present work considers the cylindrical sample of liquid iron containing initially 0.002 mass % of oxygen. This sample is placed in the crucible. The geometry of the

system is shown in Fig. 5. It is assumed, that the sample is cooled only at its vertical wall. The crucible bottom and the liquid metal surface are assumed adiabatic, for the sake of numerical solution stability. The crystallization front develops towards the centre of the sample.

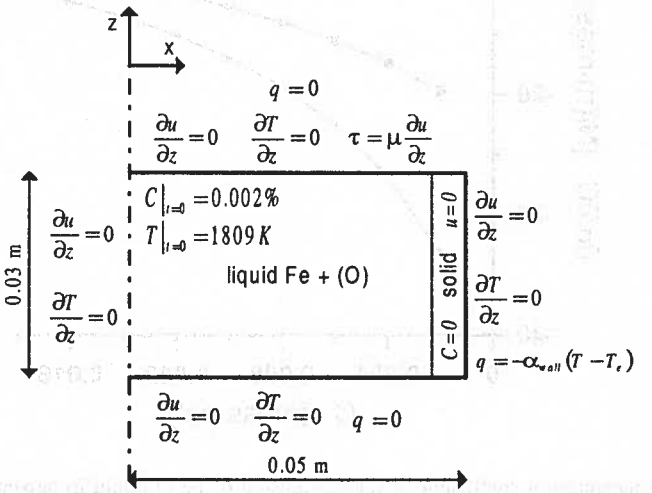

Fig. 5. The sample under consideration (calculation domain) and the boundary conditions

Due to the low value of distribution coefficient of oxygen in steel, its concentration at the front region (C_i) strongly increases [5], according to equation (4):

$$C_i = \frac{C(t)_{x=0}}{k}. \tag{4}$$

The maximum concentration of oxygen, i.e. solubility limit, is temperature dependent according to [6] — equation (5):

$$\lg [\%O]_{sat} = 2.734 - \frac{6329}{T}. \tag{5}$$

At the melting temperature of steel 1808 K the oxygen solubility is 0.17 mass %. Thus the additional condition demands, that C_i value does not exceed the solubility limit. The liquid metal is assumed as slightly compressible[1)] Newtonian liquid, what allows to describe the process by means of the set of following equations:

- continuity

$$\frac{\partial \rho}{\partial t} + \nabla(\rho \bar{u}) = 0 \tag{6}$$

- momentum conservation (Navier-Stokes)

$$\frac{\partial \bar{u}}{\partial t} + \bar{u} \cdot \nabla \bar{u} = -\frac{1}{\rho} \nabla p + \frac{\mu}{\rho} \nabla^2 \bar{u} + \beta \Delta T \cdot \bar{g} \tag{7}$$

[1)] Density ρ is a function of temperature

- thermal energy conservation,

$$\frac{\partial T}{\partial t} + \bar{u} \cdot \nabla T = \frac{\lambda}{\rho \cdot c_p} \nabla^2 T \tag{8}$$

- oxygen balance in diffusive-convective flow

$$\frac{\partial C}{\partial t} + \bar{u} \cdot \nabla C = D \nabla^2 C, \tag{9}$$

where:
$\bar{u}$ — the velocity vector.

The effect of surface convection was taken into account as the boundary condition expressing the shear stress at the free surface:

$$\tau = \mu \frac{\partial u}{\partial z} = \left(\frac{\partial \sigma}{\partial T} \cdot \frac{\partial T}{\partial x} \right)_C + \left(\frac{\partial \sigma}{\partial C} \cdot \frac{\partial C}{\partial x} \right)_T. \tag{10}$$

The geometry of the system and the boundary conditions as well as initial conditions at the boundary surfaces are presented in Fig. 5. The material parameters of iron and the conditions of solidification are presented in Table 1.

TABLE 1

Physical properties of iron and initial conditions of crystallization process

Viscosity, μ	$5.023 \cdot 10^3$ kg/(m /· s)	[7]
Density of liquid, ρ_L	7030 kg/m^3	[8]
Density of solid, ρ_S	7350 kg/m^3	[8]
Heat capacity of liquid, c_{pl}·	824 J/(kg·K)	[8]
Heat capacity of solid, c_{pS}	750 J/(kg·K)	[8]
Thermal conductivity of liquid, Λ_L	36 W/(m·K)	[8]
Thermal conductivity of solid, Λ_S	38 W/(m·K)	[8]
Thermal expansion coefficient, β	$1.25 \cdot 10^{-4}$	[9]
Melting point, T_m	1808 K	[9]
Heat of melting, H_m	$247 \cdot 10^3$ J/kg	[10]
Heat exchange coefficient at the crucible wall, α_{wall}	3.780 W/(m^2·K)	
Diffusion coefficient of oxygen, D	$1.5 \cdot 10^{-8}$m^2/s	[9]
Equilibrium distribution coefficient of oxygen, k	0.022	[9]
External temperature, T_e	293 K	
Initial temperature of iron in crucible, $T\|_{t=0}$	1809 K	
Initial oxygen concentration in liquid iron, $C\|_{t=0}$	0.002 wt pct	

At the inter-phase boundary the solid phase is transferred to liquid at the constant temperature 1808 K. In this case Stefan boundary condition was assumed ($T_L = T_S$) [11]:

$$-\lambda_L \frac{\partial T_L}{\partial x} = -\lambda_S \frac{\partial T_S}{\partial x} + \rho \cdot H_m \frac{\partial x}{\partial t}. \tag{11}$$

The density ρ in equation (10) regards the appropriate phase (ρ_S for solid and ρ_L for liquid). The influence of oxygen concentration on liquid iron density is negligible, and it is not considered in calculations. It was also assumed that at the crystallization front the oxygen diffusion in liquid fulfills the boundary conditions:

$$-D\frac{\partial C(x,t)}{\partial x} = (1-k) \cdot \frac{\partial x_i}{\partial t} \cdot C_i(x,t) \tag{12}$$

$$D\frac{\partial C(z,t)}{\partial z} = (1-k) \cdot \frac{\partial z_i}{\partial t} \cdot C_i(z,t), \tag{13}$$

where:
C_i — the oxygen concentration in liquid iron at the crystallization front at the time t,
x_i — the tangent coordinate of the position of crystallization front at the time t,
z_i — the axial coordinate of the position of crystallization front at the time t,
k — the equilibrium distribution coefficient of oxygen.

4. Results of numerical calculations and discussion

The problem presented above was solved by means of the finite elements method with the use of ADINA-F® program. The 2D area of one-half of vertical sample section was covered with the grid of 4200 three-node finite elements. The numerical simulation of 2D axi-symmetrical problem was carried out under the assumption, that the considered area has the initial properties corresponding to liquid Fe-O solution at the temperature 1809 K. As a result of numerical calculations, the temperature, concentration and velocity fields were determined as a function of time.

It must be noted, that the process of crystallization is slow, as it is caused by 1 K difference of temperature. The average velocity of solidification front is $3 \cdot 10^{-6}$ m/s. The calculated tangent velocity component of surface flow has the maximum value 0.0084 m/s. In such circumstances the flow may be certainly assumed as laminar.

The examples of obtained results are presented in Figs. 6 – 11. Fig. 6 demonstrates, how the distribution of oxygen at free surface of the sample varies with the course of the process. The strong increase in the region of crystallization front may be observed. In the remaining part of surface (more than 90%) the oxygen concentration is almost constant and it slowly increases with time. Total amount of oxygen in the sample is constant, so its level in remaining part of liquid sample slightly increases due to gradual reduction of the liquid part volume.

Fig. 7 presents the tangent (horizontal) component of metal velocity along its free surface at three chosen times of process duration. At major part of the surface the flow is directed outwards from the center. The high peak on velocity curve is observed

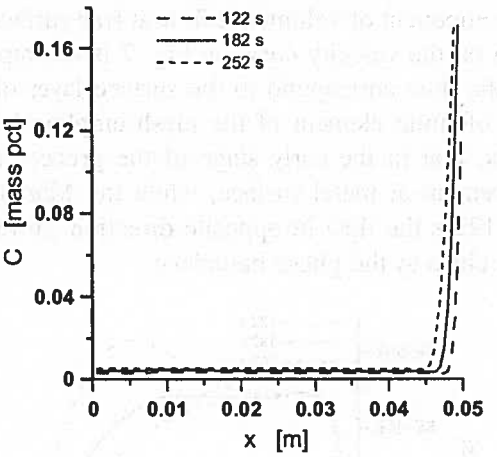

Fig. 6. The distribution of oxygen concentration at the free surface of liquid metal

close to the sample axis of symmetry, while exactly at the axis its value is zero. This maximum is the result of a sample geometry. In the surface region close to the inter-phase boundary the horizontal component of the surface velocity has the opposite direction (towards the sample center), what is evidently the result of Marangoni flow. This part of the velocity plot is shown in extension in Fig. 7. It was calculated, that the flow in opposite direction appears after 122 s. This corresponds to the oxygen concentration 0.132 mass % in the liquid.

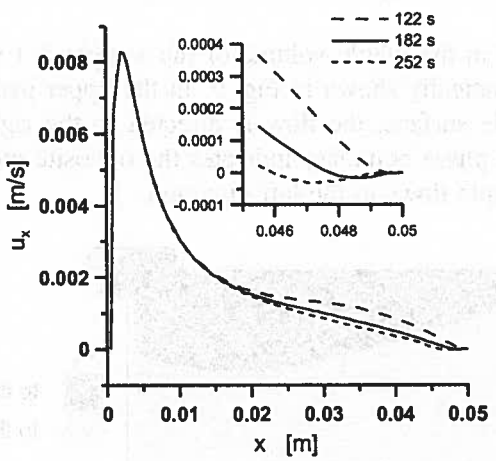

Fig. 7. The tangent (horizontal) component of metal velocity at its free surface

It may be easily deduced, that in the case of cylindrical sample the flow velocity is not the proper measure of the mass transfer in the whole sample volume and it should be replaced with the volumetric or mass flow. This was shown in Fig. 8, where the

tangent (horizontal) component of volumetric flow at free surface of metal is presented. The strong maximum on the velocity curve in Fig. 7 is not reproduced in Fig. 8. The numerical values of the flow correspond to the surface layer of the thickness $5 \cdot 10^{-4}$ m, which is the size of finite element of the mesh employed in the present work. It follows from this plot, that in the early stage of the process the thermal convection causes the rapid movement at metal surface, while the Marangoni convection is not developed yet. After 122 s the flow in opposite direction (towards the sample center) appears in the region close to the phase boundary.

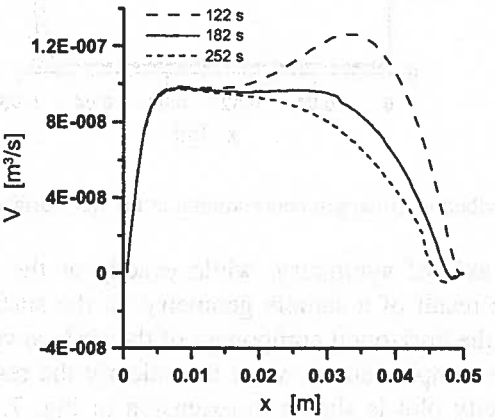

Fig. 8. The tangent (horizontal) component of the volumetric flow at free surface of metal (numerical values correspond to surface layer thickness $5 \cdot 10^{-4}$ m)

The flow pattern in the whole volume of the sample at t = 182 s (early stage of the process) is schematically shown in Fig. 9. In the upper part of the sample, which contains almost whole surface, the flow is directed to the right. Only small surface fragment close to the phase boundary indicates the opposite movement direction. The lower part of the sample flows to the left direction.

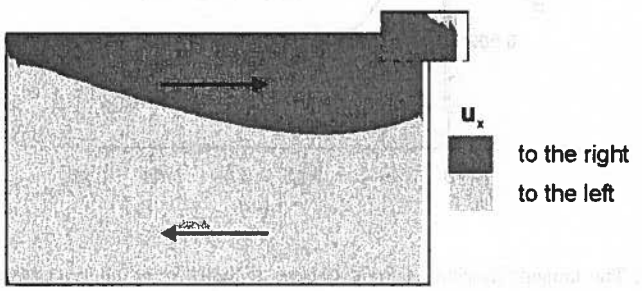

Fig. 9. Direction of convective flow in liquid sample after 182 s

The contribution of the surface (Marangoni) convection in the total convective flow in the inter-phase boundary region may be visualized in the Fig. 10, which shows the distribution of horizontal component of surface velocity calculated for three cases:

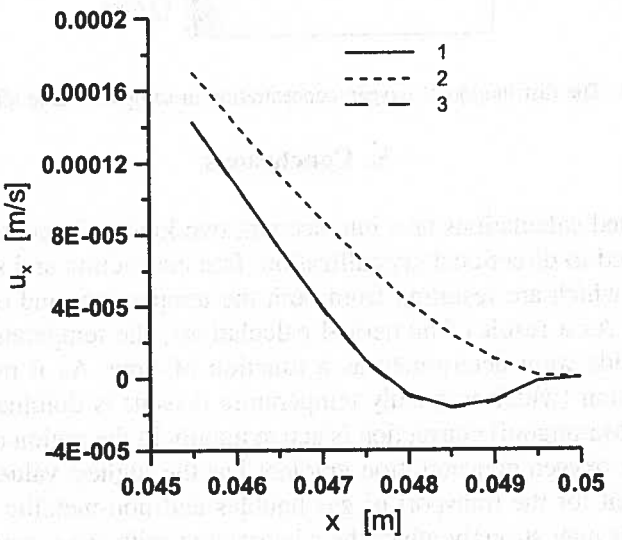

Fig. 10. The tangent velocity distribution in the neighbourhood of freezing front at hypothetical limiting conditions: 1. Thermal convection excluded, 2. Concentration convection excluded, 3. Both kinds of convection operating together

1. thermal convection excluded (constant liquid density),
2. concentration convection excluded (constant surface tension).
3. both kinds of convection operating simultaneously.

It is surprising, that in the cases 1 and 3 very similar courses of horizontal velocity are obtained. This means, that in the boundary region the concentration driven convection is dominant.

Fig. 11 shows the distribution of oxygen concentration in the sample at the initial stage of crystallization (182 s). It may be noticed that in the bottom zone of the liquid the transport of oxygen from freezing front towards the center of sample is stronger than in the surface region. This phenomenon may be explained as a result of a larger advance of freezing front in a bottom zone, and consequently larger amount of released oxygen.

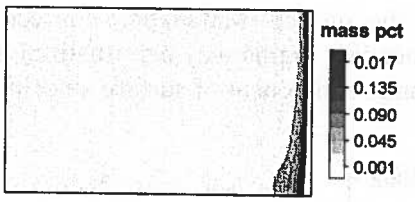

Fig. 11. The distribution of oxygen concentration in sample volume after 182 s

5. Conclusions

The presented calculations take into account two kinds of a convective flow in liquid iron subjected to directional crystallization: free convection and surface (Marangoni) convection, which are resulting from both the temperature and concentration field non-uniformity. As a result of numerical calculations, the temperature, concentration and velocity fields were determined as a function of time. As it might be expected, the free convection (which is mainly temperature driven) is dominant. Concentration driven surface (Marangoni) convection is active mainly in the region of a crystallization front, where the oxygen concentration gradient has the highest value. This occurrence may be important for the transport of gas bubbles and non-metallic inclusions during crystallization. It may strongly affect their interaction with the moving front.

The analysis presented in the present work is confined to the early stages of the solidification process, where the contribution of Marangoni flow is meaningful. The oxygen concentration gradient at the free surface, which is the driving force for this flow, tends to decrease with the crystallization progress. The maximum oxygen solubility at the assumed temperature is 0.172 mass pct. and this value limits the concentration gradient.

The contribution of Marangoni flow to total mass and heat transfer is strongly dependent on the geometry of the liquid bath, i.e. the surface to volume ratio. Generally, this contribution is small in relation to the whole volume of the sample, but considerable in relation to the surface zone.

The work was executed in frames of research project sponsored by the Ministry of Scientific Research and Information Technology, grant No 3 T08B 044 26.

REFERENCES

[1] J. Wypartowicz, R. Rejszek, Metallurgy and Foundry Engineering **30** (1), 31-41 (2004).

[2] R. Rejszek, J. Wypartowicz, Dissolution of nitrogen in liquid iron with the contribution of surface convection, XIV Intern. Sci. Conf. Iron and Steelmaking, Mala Lucivna 13-15. 10.2004.- Acta Metallurgica Slovaka (w druku).

[3] Y. Chung, A.W. Cramb, Met. Trans. B **31B**, 957-971 (2000).
[4] G.R. Belton, Met. Trans. B **7B**, 35-42 (1976).
[5] E. Fraś, Krystalizacja metali, PWN Warszawa, (2003).
[6] L. Coudurier, D.W. Hopkins, I. Wilkomirsky, Fundamentals of Metallurgical Processes, Pergamon Press 1978.
[7] N. Hirashima, R.T.C. Choo, J.M. Toguri, K. Mukai, Metallurgical and Materials Transactions B **26B**, 971-980 (1995).
[8] K.C. Mills, Recommended values of thermophysical properties for selected commercial alloys, Woodhead Publishing Limited, Abington Hall, Abington, Cambridge (2002).
[9] K. Nakajima, S. Yasuhiro, S. Mizoguchi, N. Imaishi, Metallurgical and Materials Transactions B **34B**, 37-49 (2003).
[10] H.G. Fan, H.L. Tsai, S.J. Na, Heat and Mass Transfer **44**, 417-428 (2001).
[11] B. Mochnacki, J.S. Suchy, Modelowanie i symulacja krzepnięcia odlewów, PWN Warszawa (1993).

Received: 20 June 2005.